

# Structure of the Dicobalt "Face-to-Face" Porphyrin with Two Four-Atom Amide Bridges: $\text{Co}_2(\text{FTF4}) \cdot \text{CH}_3\text{OH} \cdot 1.6\text{CH}_2\text{Cl}_2$

Kimoon Kim,<sup>†,‡</sup> James P. Collman,<sup>\*,†</sup> and James A. Ibers<sup>\*,†</sup>

Contribution from the Departments of Chemistry, Northwestern University, Evanston, Illinois 60208, and Stanford University, Stanford, California 94305.  
Received October 19, 1987

**Abstract:** The structure of the dicobalt "face-to-face" porphyrin with two four-atom amide bridges [ $\text{Co}_2(\text{FTF4})$ ] has been determined by single-crystal X-ray diffraction methods. This compound is the first synthetic molecule that catalyzes the direct four-electron reduction of  $\text{O}_2$  to  $\text{H}_2\text{O}$  in acidic media. The  $\text{Co}_2(\text{FTF4})$  molecule exhibits crystallographically imposed twofold symmetry, and hence the amide bridge is disordered. The crystal is composed of only one enantiomeric pair, d,l-anti. The two porphyrin rings of the compound are stacked almost exactly over each other; the shear displacement of the two metal centers is only 0.13 Å. These two porphyrin rings, interplanar distance 3.54 Å, are twisted by approximately 40° with respect to each other. The cobalt atom is slightly displaced out of the mean porphyrin plane toward the diporphyrin cavity and the Co-Co distance is 3.417 (4) Å. This structure is compared with those of other cofacial porphyrin dimers. Possible  $\text{O}_2$  binding modes in this compound are also discussed. Crystallographic data: monoclinic,  $C2/c$ ,  $Z = 4$ ,  $a = 14.365$  (9) Å,  $b = 14.923$  (10) Å,  $c = 27.182$  (18) Å,  $\beta = 95.94$  (1)°,  $V = 5795$  Å<sup>3</sup> at -150 °C, 2971 unique data, 215 variables,  $R(F)$  ( $F_o^2 > 3\sigma(F_o^2)$ ) = 0.084.

"Face-to-face" (FTF) porphyrins—dimeric porphyrins in which two porphyrin rings are covalently linked in a cofacial orientation—have received great attention since Collman et al.<sup>1</sup> first proposed their use as binuclear multielectron redox catalysts for small molecules such as  $\text{O}_2$  and  $\text{N}_2$ . Indeed, the dicobalt derivative of the  $\beta$ -linked porphyrin dimer with two four-atom amide bridges ( $\text{Co}_2(\text{FTF4})$ ) (Figure 1) became the first synthetic molecule to catalyze the direct four-electron ( $4e^-$ ) reduction of  $\text{O}_2$  to  $\text{H}_2\text{O}$  in strongly acidic media.<sup>2</sup> It was subsequently demonstrated that such four-electron catalytic activity is extremely sensitive to the catalyst geometry.<sup>2a,b,3</sup> Structural information concerning the cofacial porphyrins is thus very important in understanding the mechanism of catalytic  $\text{O}_2$  reduction and in the design of better catalysts. Despite considerable effort, attempts to grow crystals of various FTF4 complexes suitable for X-ray analysis were unsuccessful. Part of the difficulty may be attributed to the presence of more than one stereoisomer. The FTF4 dimer can exist in two diastereomeric forms, syn and anti (Figure 1), each as a racemic mixture. The reported synthetic procedure for free base FTF4 had been thought<sup>2b,4</sup> to yield only one diastereomer (anti), but a careful inspection of the <sup>1</sup>H NMR spectra (for example, Figures 6 and 7 in ref 3) revealed that the other diastereomer constitutes between 8 and 15% of each batch of  $\text{H}_4(\text{FTF4})$ .<sup>5</sup>

Recently, Fillers et al.<sup>6</sup> reported the X-ray crystal structures of cofacial diporphyrins held by rigid aromatic groups where the spacer is anthracene in  $\text{Ni}_2(\text{DPA})$  and biphenylene in  $\text{Cu}_2(\text{DPB})$ . The dicobalt derivatives of these diporphyrins are also efficient four-electron catalysts for  $\text{O}_2$  reduction.<sup>7</sup> This report stimulated us to resume our efforts to grow single crystals of FTF4; herein we report the X-ray crystal structure of  $\text{Co}_2(\text{FTF4})$ .

## Experimental Section

Free base  $\text{H}_4(\text{FTF4})$  and its dicobalt derivative were synthesized as described previously.<sup>4</sup> Dark purple crystals of  $\text{Co}_2(\text{FTF4})$  suitable for X-ray analysis were grown by slow diffusion of methanol into a dichloromethane solution of the porphyrin complex. Since solvate loss occurred rapidly on exposure to air at room temperature, the crystals were coated with Paraton N (a mixture of long alkyl chain hydrocarbons from Exxon Chemical) before being mounted on a glass fiber and transferred quickly to the cold stream (-150 °C) of an Enraf-Nonius CAD4 diffractometer. Unit cell parameters were determined by least-squares refinement of 25 reflections ( $10.0^\circ < \theta$  (Mo K $\alpha$ )  $< 11.7^\circ$ ) that had been automatically centered on the diffractometer. A preliminary intensity check suggested that the crystals belong to either space group  $Cc$  or  $C2/c$  of the monoclinic system. Data collection was performed at

-150 °C. No systematic changes were observed in the intensities of six standard reflections that were measured every 3 h of X-ray exposure. Crystallographic details are given in Table I.

Standard procedures and programs were used to develop and refine the structure.<sup>8</sup> The position of the cobalt atom was obtained from a Patterson map. The remaining atoms belonging to the molecule were located by the direct methods program DIRDIF.<sup>9</sup> An analytical absorption correction was applied to the intensity data and the equivalent reflections were averaged. The centrosymmetric space group  $C2/c$  was assumed, as averaging of these Friedel pairs,  $hkl$  and  $\bar{h}\bar{k}\bar{l}$ , that are non-equivalent in the noncentrosymmetric space group  $Cc$  led to an  $R$  index for averaging of 3.2%. The  $\text{Co}_2(\text{FTF4})$  molecule shows crystallographically imposed twofold symmetry: one porphyrin ring and two half-amide (disordered) bridges belong to the asymmetric unit. After a least-squares refinement, in a difference electron density map a methanol solvate was detected near an amide bridge. After several cycles of refinement of the structure large peaks near an inversion center in a difference electron density map were interpreted in terms of two disordered dichloromethane molecules. Owing to the small number of data with  $I > 3\sigma(I)$ , only cobalt and chlorine atoms were refined anisotropically. Most hydrogen atoms of the methyl groups were located in difference electron density maps. Idealized hydrogen atom positions ( $\text{C-H} = 0.95$  Å,  $\text{H-C-H} = 109.5^\circ$ ) were either calculated (non-methyl) or obtained from a least-squares adjustment of the observed position (methyl) and were added as fixed contributions to the structure factors. Each hydrogen atom was assigned an isotropic thermal parameter 1 Å<sup>2</sup> greater than that of the atom to which it is attached. Solvent hydrogen atoms were not included

(1) (a) Collman, J. P.; Elliott, C. M.; Halbert, T. R.; Tovrog, B. S. *Proc. Natl. Acad. Sci. U.S.A.* 1977, 74, 18-22. (b) For a review see: Collman, J. P.; Anson, F. C.; Bencosme, C. S.; Chong, A.; Collins, T.; Denisevich, P.; Evitt, E.; Geiger, T.; Ibers, J. A.; Jameson, G.; Konai, Y.; Koval, C.; Meier, K.; Oakley, R.; Pettman, R.; Schmittou, E.; Sessler, J. In *Organic Synthesis Today and Tomorrow*; Trost, B. M., Hutchinson, C. R., Eds.; Pergamon: Oxford, 1981; pp 29-45.

(2) (a) Collman, J. P.; Marrocco, M.; Denisevich, P.; Koval, C.; Anson, F. C. *J. Electroanal. Chem.* 1979, 101, 117-122. (b) Collman, J. P.; Denisevich, P.; Konai, Y.; Marrocco, M.; Koval, C.; Anson, F. C. *J. Am. Chem. Soc.* 1980, 102, 6027-6036. (c) Liu, H. Y.; Weaver, M. J.; Wang, C.-B.; Chang, C. K. *J. Electroanal. Chem.* 1983, 145, 439-447.

(3) Durand, R. R.; Bencosme, C. S.; Collman, J. P.; Anson, F. C. *J. Am. Chem. Soc.* 1983, 105, 2710-2718.

(4) Collman, J. P.; Anson, F. C.; Barnes, C. E.; Bencosme, C. S.; Geiger, T.; Evitt, E. R.; Kreh, R. P.; Meier, K.; Pettman, R. G. *J. Am. Chem. Soc.* 1983, 105, 2694-2699.

(5) Kim, K. Ph.D. Thesis, Stanford University, 1986, pp 15-18.

(6) Fillers, J. P.; Ravichandran, K. G.; Abadalmuhdi, I.; Tulinsky, A.; Chang, C. K. *J. Am. Chem. Soc.* 1986, 108, 417-424.

(7) Chang, C. K.; Liu, H. Y.; Abdalmuhdi, I. *J. Am. Chem. Soc.* 1984, 106, 2725-2726.

(8) For example: Waters, J. M.; Ibers, J. A. *Inorg. Chem.* 1977, 16, 3273-3277.

(9) DIRDIF: Direct methods applied to Difference structure factors to strengthen Fourier methods. Beurskens, P. T.; Bosman, W. P.; Doesburg, H. M.; Gould, R. O.; van den Hark, Th. E. M.; Prick, P. A. *J. Computational Crystallography*; Sayre, D., Ed.; Clarendon Press: Oxford, 1982; p 516.

<sup>†</sup> Northwestern University.

<sup>‡</sup> Stanford University.

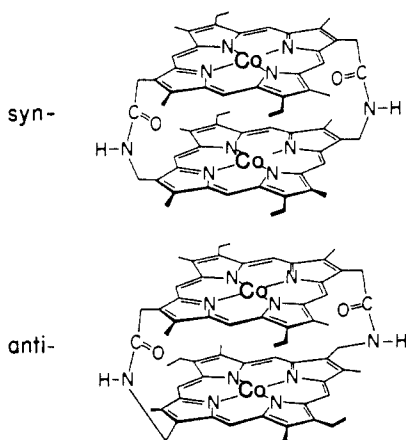


**Figure 1.** Syn and anti diastereomers of  $\text{Co}_2(\text{FTF4})$ . Other enantiomers are not shown.

**Table I.** Crystallographic Data for  $\text{Co}_2(\text{FTF4})\cdot\text{CH}_3\text{OH}\cdot 1.6\text{CH}_2\text{Cl}_2$

formula	$\text{Co}_2\text{C}_{62}\text{H}_{62}\text{N}_{10}\text{O}_2\cdot\text{CH}_4\text{O}\cdot 1.6\text{CH}_2\text{Cl}_2$
formula wt.	1265.05
space group	$C_{2h}^2-C2/c$
$a$ , Å	14.365 (9)
$b$ , Å	14.923 (10)
$c$ , Å	27.182 (18)
$\beta$ , deg	95.94 (1)
vol, Å <sup>3</sup>	5795
$Z$	4
temp, °C	-150 <sup>a</sup>
density (calcd), g/cm <sup>3</sup>	1.450
crystal planes	{100} (0.075), {001} (0.230), {111} (0.15) <sup>b</sup>
crystal vol, mm <sup>3</sup>	0.0021
radiation	graphite monochromated Mo $K\alpha$ ( $\lambda(K\alpha_1) = 0.7093$ Å)
linear abs coeff, cm <sup>-1</sup>	7.75
transmission factors	0.923-0.959
detector aperture	3.5 mm wide $\times$ 4.0 mm high
	17 cm from crystal
take-off angle, deg	3.4
scan mode	$\omega$ scan
scan speed, deg/min	2.06; for reflns with $I < 3\sigma(I)$ rescans were forced to achieve $I > 3\sigma(I)$ , up to 100 s total scan time
$2\theta$ limits	$4.0 \leq 2\theta \leq 41.0$
bkgd counts	$1/4$ of scan range on each side of refltn
scan width, deg	$\pm 1.1$ in $\omega$
data collected	$\pm h, \pm k, \pm l$ ( $4.0 \leq 2\theta \leq 20.0$ ) $\pm h, \pm k, \pm l$ ( $20.0 < 2\theta \leq 41.0$ )
unique data	2971
unique data with $F_o^2 > 3\sigma(F_o^2)$	1206
no. of variables in final refinement	215
$R(F^2)$	0.162
$R_w(F^2)$	0.187
$R(F)$ ( $F_o^2 > 3\sigma(F_o^2)$ )	0.084
$R_w(F)$ ( $F_o^2 > 3\sigma(F_o^2)$ )	0.077
error in observation of unit wt, e <sup>2</sup>	1.16

<sup>a</sup>The low-temperature system is from a design by Prof. J. J. Bonnet and S. Askenazy and is commercially available from Sotarem, Z. I. de Vic, 31320 Castanet-Tolosan, France. <sup>b</sup>The numbers in parentheses are the distances in mm between Friedel pairs of the preceding form.

in this model. The final cycle of refinement on  $F^2$ , involving all 2971 unique data and 215 variables, gave  $R(F^2)$  and  $R_w(F^2)$  values of 0.162 and 0.187, respectively. The conventional  $R$  indices on  $F$  for 1206 reflections having  $F_o^2 > 3\sigma(F_o^2)$  are  $R(F_o) = 0.084$  and  $R_w(F_o) = 0.077$ , the occupancy factor of solvent S3 refined to 0.30 (2). That of solvent S1 was fixed at 0.50, its maximum value in view of the disorder of the bridge, as earlier refinements had led to values near 0.5. The occupancy of solvent S1 was also fixed at 0.50, since it is disordered over a center of inversion and cannot exceed one-half occupancy. Earlier refinement had similarly led to an occupancy near 0.5. In the final difference electron density map the largest peak (1.2 (3) e Å<sup>-3</sup>) is near the amide bridge I and the second largest (1.0 (3) e Å<sup>-3</sup>) is near the amide bridge

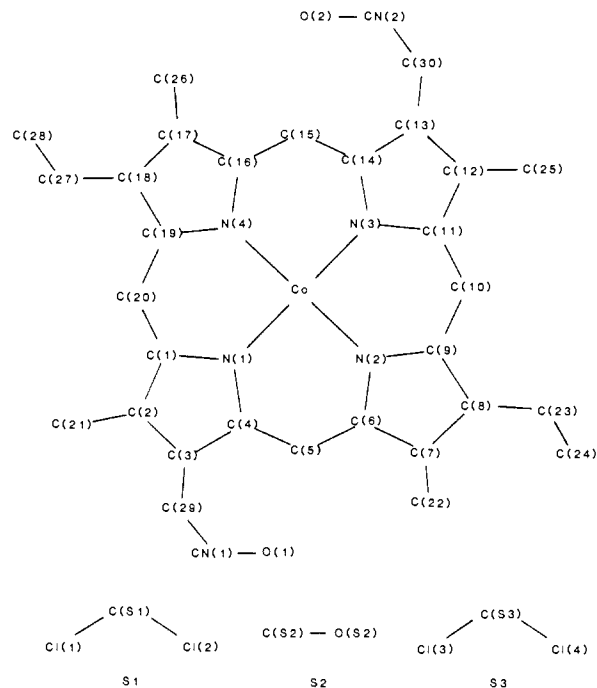


**Figure 2.** Atom-labeling scheme for  $\text{Co}_2(\text{FTF4})\cdot\text{CH}_3\text{OH}\cdot 1.6\text{CH}_2\text{Cl}_2$ .

II. These are to be compared with a height of about  $5.4 \text{ e Å}^{-3}$  for a typical C atom in the structure.

The atom-labeling scheme for the  $\text{Co}_2(\text{FTF4})$  molecule and solvates is given in Figure 2 where CN(1) and CN(2) are both half-carbon and half-nitrogen, and O(1) and O(2) are both half-occupied. The positional parameters and equivalent isotropic thermal parameters for non-hydrogen atoms are listed in Table SI.<sup>10</sup> The anisotropic thermal parameters, the hydrogen atom parameters, and the final values of  $10|F_o|$  versus  $10|F_c|$  are given in Tables SII, SIII, and SIV, respectively.<sup>10</sup>

## Results

A stereoview of the structure of  $\text{Co}_2(\text{FTF4})$  is shown in Figure 3. The  $\text{Co}_2(\text{FTF4})$  molecule exhibits crystallographically imposed twofold symmetry and has disordered bridges, the midpoints of which define the twofold axis. Although the starting powder sample contains ca. 10% of the minor isomer (syn), the crystal appears to be composed of only one enantiomeric pair, d,l-anti.

One of the striking features of the structure is that the two porphyrin rings are stacked almost exactly over each other (Figure 4). The Co-Co distance is 3.417 (4) Å and the lateral displacement or slippage of the two Co atoms is only 0.13 Å which corresponds to a slip angle<sup>11</sup> of 2.2°. This result is in agreement with a slip angle of  $15 \pm 10^\circ$  found in a recent EPR spectroscopic study<sup>12</sup> on a very similar molecule<sup>13</sup> in frozen solution. The mean interplanar distance between the two porphyrin rings, which are essentially parallel (dihedral angle =  $0.24^\circ$ , Table SV<sup>10</sup>), is 3.54 Å corresponding to a normal van der Waals' contact. The two porphyrin rings are twisted by approximately  $40^\circ$  with respect to one another (torsion angle N(1)-Co-Co'-N(1)' is  $41.3 (6)^\circ$ ).

Both amide bridges are nearly planar: the mean deviations from the planes are 0.21 and 0.17 Å for amides I and II, respectively. The two amide planes are parallel to each other and almost perpendicular to the mean porphyrin planes (Table SV<sup>10</sup>). Owing to the disorder, some bond parameters, especially bond distances, for the amide bridges (see Tables II and III) deviate significantly from those for normal peptide bonds.<sup>14</sup> For example, bond

(10) Supplementary material.

(11) In this study the slippage of the two Co atoms is defined as the lateral displacement of one Co center relative to the other in a direction parallel to the 24-atom least-squares porphyrin plane. Slip angle =  $\sin^{-1}$  (slippage/metal-metal distance).

(12) Eaton, S. S.; Eaton, G. R.; Chang, C. K. *J. Am. Chem. Soc.* **1985**, *107*, 3177-3184.

(13) The porphyrin dimer used in ref 12 has *n*-pentyl groups where ethyl groups are located in FTF4.

(14) Schulz, G. E.; Schirmer, R. H. *Principles of Protein Structure*; Springer-Verlag: New York, 1979; p 18.

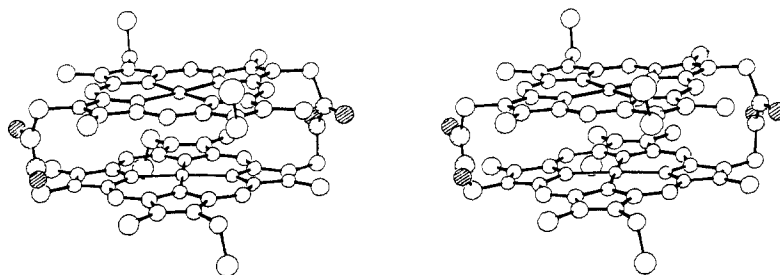


**Figure 3.** Stereodiagram of  $\text{Co}_2(\text{FTF4})$ . The disorder of the amide groups is shown. Circles with dots indicate half-carbon and half-nitrogen atoms, while hatched circles indicate half-occupied oxygen atoms. Hydrogen atoms are omitted for the sake of clarity.

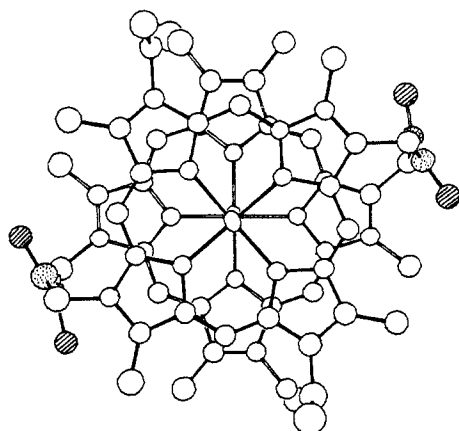


**Figure 4.** Drawings of the  $\text{Co}_2(\text{FTF4})$  molecule viewed perpendicular to the porphyrin planes.

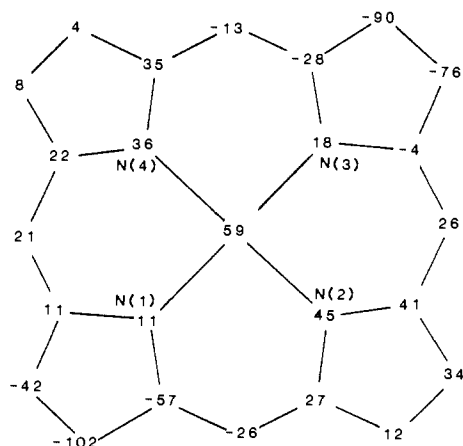


**Figure 5.** Displacements (in  $\text{\AA} \times 10^3$ ) of atoms from the least-squares plane of the 24-atom porphyrin skeleton. The estimated standard deviations are 0.009  $\text{\AA}$  for nitrogen atoms and 0.011 or 0.012  $\text{\AA}$  for carbon atoms.

distances  $\text{CN}(1)\text{-O}(1)$  (1.326 (19)  $\text{\AA}$ ) and  $\text{CN}(2)\text{-O}(2)$  (1.390 (19)  $\text{\AA}$ ) are too long for a normal  $\text{C}=\text{O}$  bond (1.24  $\text{\AA}$ ), while bond distances  $\text{CN}(1)\text{-CN}(1)'$  (1.283 (20)  $\text{\AA}$ ) and  $\text{CN}(2)\text{-CN}(2)'$  (1.223 (22)  $\text{\AA}$ ) are too short for a normal  $\text{C-N}$  bond (1.32  $\text{\AA}$ ). However, no unusual strain in the bridges is apparent and the "end-to-end" distances,  $\text{C}(29)\text{-C}(29)'$  (3.76 (3)  $\text{\AA}$ ) and  $\text{C}(31)\text{-C}(31)'$  (3.73 (3)  $\text{\AA}$ ) are not markedly different from the  $\text{C}_\alpha\text{-C}_\alpha'$  distance of a typical peptide bond, 3.80  $\text{\AA}$ .

**Porphyrin Conformation.** Bond distances and bond angles are listed in Tables II and III, respectively. The average bond parameters are typical of metalloporphyrins.<sup>15</sup> The porphyrin core is slightly domed: all the pyrrole nitrogen atoms are displaced out of the mean porphyrin plane toward the diporphyrin cavity. The deviations of the atoms from the 24-atom least-squares plane

**Table II.** Bond Distances ( $\text{\AA}$ ) for  $\text{Co}_2(\text{FTF4})\cdot\text{CH}_3\text{OH}\cdot 1.6\text{CH}_2\text{Cl}_2$

atoms	distance	atoms	distance
$\text{Co-N}(1)$	1.957 (10)	$\text{Co-N}(3)$	1.976 (10)
$\text{Co-N}(2)$	1.962 (10)	$\text{Co-N}(4)$	1.978 (10)
	av $\text{Co-N}^a$		1.968 (10)
$\text{N}(1)\text{-C}(1)$	1.367 (14)	$\text{N}(3)\text{-C}(11)$	1.389 (14)
$\text{N}(1)\text{-C}(4)$	1.394 (15)	$\text{N}(3)\text{-C}(14)$	1.377 (14)
$\text{N}(2)\text{-C}(6)$	1.381 (15)	$\text{N}(4)\text{-C}(16)$	1.392 (15)
$\text{N}(2)\text{-C}(9)$	1.380 (14)	$\text{N}(4)\text{-C}(19)$	1.397 (14)
	av $\text{N-C}_a^b$		1.385 (15)
$\text{C}(1)\text{-C}(2)$	1.445 (16)	$\text{C}(11)\text{-C}(12)$	1.447 (17)
$\text{C}(4)\text{-C}(3)$	1.447 (16)	$\text{C}(14)\text{-C}(13)$	1.432 (15)
$\text{C}(6)\text{-C}(7)$	1.447 (16)	$\text{C}(16)\text{-C}(17)$	1.443 (16)
$\text{C}(9)\text{-C}(8)$	1.431 (16)	$\text{C}(19)\text{-C}(18)$	1.461 (16)
	av $\text{C}_a\text{-C}_b$		1.444 (17)
$\text{C}(2)\text{-C}(3)$	1.311 (15)	$\text{C}(12)\text{-C}(13)$	1.355 (15)
$\text{C}(7)\text{-C}(8)$	1.359 (17)	$\text{C}(17)\text{-C}(18)$	1.325 (16)
	av $\text{C}_b\text{-C}_c$		1.338 (23)
$\text{C}(5)\text{-C}(4)$	1.366 (16)	$\text{C}(15)\text{-C}(14)$	1.357 (15)
$\text{C}(5)\text{-C}(6)$	1.361 (16)	$\text{C}(15)\text{-C}(16)$	1.378 (16)
$\text{C}(10)\text{-C}(9)$	1.377 (16)	$\text{C}(20)\text{-C}(19)$	1.358 (16)
$\text{C}(10)\text{-C}(11)$	1.357 (17)	$\text{C}(20)\text{-C}(1)$	1.364 (16)
	av $\text{C}_a\text{-C}_m$		1.365 (17)
$\text{C}(2)\text{-C}(21)$	1.515 (16)	$\text{C}(7)\text{-C}(22)$	1.497 (16)
$\text{C}(8)\text{-C}(23)$	1.523 (17)	$\text{C}(12)\text{-C}(25)$	1.475 (17)
$\text{C}(17)\text{-C}(26)$	1.495 (17)	$\text{C}(18)\text{-C}(27)$	1.500 (15)
$\text{C}(23)\text{-C}(24)$	1.540 (18)	$\text{C}(27)\text{-C}(28)$	1.525 (17)
$\text{C}(3)\text{-C}(29)$	1.510 (17)	$\text{C}(13)\text{-C}(30)$	1.539 (17)
$\text{C}(29)\text{-CN}(1)$	1.523 (16)	$\text{C}(30)\text{-CN}(2)$	1.550 (18)
$\text{CN}(1)\text{-O}(1)$	1.326 (19)	$\text{CN}(2)\text{-O}(2)$	1.390 (19)
$\text{CN}(1)\text{-CN}(1)'^c$	1.283 (20)	$\text{CN}(2)\text{-CN}(2)'$	1.223 (22)
$\text{Cl}(1)\text{-C}(S1)$	1.34 (7)	$\text{Cl}(2)\text{-C}(S1)$	1.79 (7)
$\text{Cl}(3)\text{-C}(S3)$	1.93 (8)	$\text{Cl}(4)\text{-C}(S3)$	1.88 (8)
$\text{C}(S2)\text{-O}(S2)$	1.44 (4)		

<sup>a</sup>The estimated standard deviation in parentheses is the larger of that calculated for an individual observation from the inverse matrix or on the assumption that the values averaged are from the same population. <sup>b</sup>The nomenclature is that of Hoard.<sup>15</sup> <sup>c</sup>Primed and unprimed atoms with the same label are related by the crystallographic twofold symmetry.

of the porphyrin skeleton are displayed in Figure 5. The mean deviation is 0.033  $\text{\AA}$  and the two largest deviations are 0.102 (12) and 0.090 (11)  $\text{\AA}$  for atoms  $\text{C}(3)$  and  $\text{C}(13)$ , respectively, to which the amide straps are linked. The cobalt atom is displaced 0.06  $\text{\AA}$  out of the mean porphyrin plane (0.03  $\text{\AA}$  out of the nitrogen coordination plane) toward the diporphyrin cavity. The average  $\text{Co-N}$  distance, 1.968 (10)  $\text{\AA}$ , is possibly longer than that observed for four-coordinate  $\text{Co}(\text{TPP})$ , 1.949 (1)  $\text{\AA}$ .<sup>16</sup>

**Crystal Packing.** Figure 6 illustrates the packing of  $\text{Co}_2(\text{FTF4})$  units, methanol, and disordered dichloromethane solvates. A given dimer has its porphyrin planes parallel to but slipped relative to the next dimer. The shortest inter-porphyrin distance of 3.53 (4)  $\text{\AA}$  suggests the existence of  $\pi\text{-}\pi$  interactions often observed for monomeric metalloporphyrins in the crystalline state.<sup>17</sup> The

(15) Hoard, J. L. In *Porphyrin and Metalloporphyrins*; Smith, K. M., Ed.; Elsevier: Amsterdam, 1975; pp 317-380.

(16) (a) Stevens, E. D. *J. Am. Chem. Soc.* **1981**, *103*, 5087-5095. (b) Madura, P.; Scheidt, W. R. *Inorg. Chem.* **1976**, *15*, 3182-3184.

(17) Scheidt, W. R.; Lee, Y. J. *Struct. Bonding (Berlin)* **1987**, *64*, 1-70.

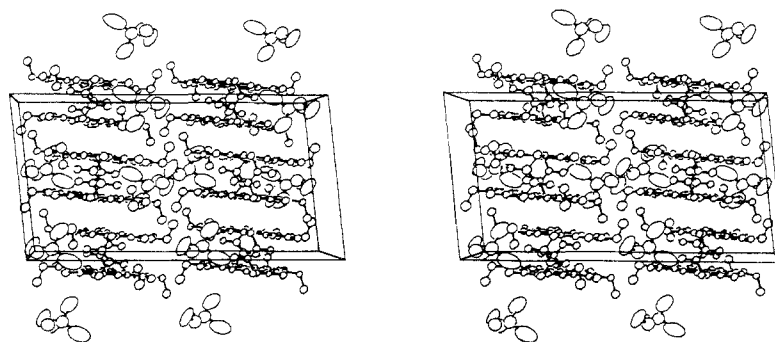


Figure 6. Crystal packing diagram for  $\text{Co}_2(\text{FTF4})\cdot\text{CH}_3\text{OH}\cdot 1.6\text{CH}_2\text{Cl}_2$  looking down the  $b$  axis.

Table III. Bond Angles (deg) for  $\text{Co}_2(\text{FTF4})\cdot\text{CH}_3\text{OH}\cdot 1.6\text{CH}_2\text{Cl}_2$

atoms	angle	atoms	angle
N(1)–Co–N(2)	90.2 (4)	N(2)–Co–N(3)	90.1 (4)
N(1)–Co–N(4)	89.3 (4)	N(3)–Co–N(4)	90.4 (4)
	av N–Co–N		90.0 (6)
N(1)–Co–N(3)	177.4 (4)	N(2)–Co–N(4)	178.8 (4)
	av N–Co–N		178.1 (10)
Co–N(1)–C(1)	128.4 (9)	Co–N(3)–C(11)	127.5 (9)
Co–N(1)–C(4)	128.2 (9)	Co–N(3)–C(14)	127.4 (9)
Co–N(2)–C(6)	127.2 (9)	Co–N(4)–C(16)	127.3 (9)
Co–N(2)–C(9)	128.6 (9)	Co–N(4)–C(19)	127.9 (9)
	av Co–N–C <sub>a</sub>		127.8 (9)
N(1)–C(1)–C(2)	111.2 (11)	N(3)–C(11)–C(12)	111.0 (12)
N(1)–C(4)–C(3)	110.9 (12)	N(3)–C(14)–C(13)	109.9 (12)
N(2)–C(6)–C(7)	110.8 (12)	N(4)–C(16)–C(17)	111.7 (12)
N(2)–C(9)–C(8)	112.0 (13)	N(4)–C(19)–C(18)	108.1 (12)
	av N–C <sub>a</sub> –C <sub>b</sub>		110.7 (13)
C(1)–N(1)–C(4)	103.4 (10)	C(11)–N(3)–C(14)	105.1 (11)
C(6)–N(2)–C(9)	104.1 (11)	C(16)–N(4)–C(19)	104.8 (11)
	av C <sub>a</sub> –N–C <sub>a</sub>		104.4 (11)
C(1)–C(2)–C(3)	107.8 (13)	C(11)–C(12)–C(13)	105.2 (13)
C(2)–C(3)–C(4)	106.6 (12)	C(12)–C(13)–C(14)	108.7 (12)
C(6)–C(7)–C(8)	106.8 (13)	C(16)–C(17)–C(18)	105.5 (12)
C(7)–C(8)–C(9)	106.2 (13)	C(17)–C(18)–C(19)	109.9 (13)
	av C <sub>a</sub> –C <sub>b</sub> –C <sub>b</sub>		107.1 (16)
N(1)–C(1)–C(20)	125.3 (12)	N(3)–C(11)–C(10)	123.4 (13)
N(1)–C(4)–C(5)	123.2 (12)	N(3)–C(14)–C(15)	124.5 (12)
N(2)–C(6)–C(5)	124.9 (13)	N(4)–C(16)–C(15)	123.3 (13)
N(2)–C(9)–C(10)	122.6 (13)	N(4)–C(19)–C(20)	123.9 (13)
	av N–C <sub>a</sub> –C <sub>m</sub>		123.9 (13)
C(2)–C(1)–C(20)	123.5 (12)	C(12)–C(11)–C(10)	125.6 (13)
C(3)–C(4)–C(5)	125.8 (13)	C(13)–C(14)–C(15)	125.6 (12)
C(7)–C(6)–C(5)	124.2 (13)	C(17)–C(16)–C(15)	124.8 (13)
C(8)–C(9)–C(10)	125.4 (14)	C(18)–C(19)–C(20)	128.0 (13)
	av C <sub>b</sub> –C <sub>a</sub> –C <sub>m</sub>		125.4 (14)
C(4)–C(5)–C(6)	126.1 (13)	C(14)–C(15)–C(16)	127.0 (13)
C(9)–C(10)–C(11)	127.7 (14)	C(19)–C(20)–C(1)	125.3 (13)
	av C <sub>a</sub> –C <sub>m</sub> –C <sub>a</sub>		126.5 (14)
C(1)–C(2)–C(21)	124.7 (12)	C(11)–C(12)–C(25)	129.7 (14)
C(3)–C(2)–C(21)	127.5 (14)	C(13)–C(12)–C(25)	125.0 (13)
C(2)–C(3)–C(29)	130.6 (14)	C(12)–C(13)–C(30)	127.5 (13)
C(4)–C(3)–C(29)	122.5 (13)	C(14)–C(13)–C(30)	123.6 (12)
C(6)–C(7)–C(22)	124.9 (12)	C(16)–C(17)–C(26)	124.3 (13)
C(8)–C(7)–C(22)	128.2 (14)	C(18)–C(17)–C(26)	130.1 (14)
C(7)–C(8)–C(23)	128.4 (14)	C(17)–C(18)–C(27)	127.6 (13)
C(9)–C(8)–C(23)	125.1 (13)	C(19)–C(18)–C(27)	122.5 (12)
C(8)–C(23)–C(24)	112.8 (12)	C(18)–C(27)–C(28)	113.4 (11)
C(3)–C(29)–CN(1)	109.5 (11)	C(13)–C(30)–CN(2)	109.4 (11)
C(29)–CN(1)–O(1)	118.9 (12)	C(30)–CN(2)–O(2)	120.0 (12)
C(29)–CN(1)–CN(1)'	117.1 (16)	C(30)–CN(2)–CN(2)'	113.7 (18)
O(1)–CN(1)–CN(1)'	123.8 (18)	O(2)–CN(2)–CN(2)'	126.2 (20)
Cl(1)–C(S1)–Cl(2)	122.3 (47)	Cl(3)–C(S3)–Cl(4)	106.2 (43)

shortest Co–Co distance between dimer molecules is 8.437 (5) Å. The oxygen atom of the methanol solvate forms a hydrogen bond with the NH group of amide II of a dimer ( $\text{O}(\text{S}2)\cdots\text{CN}(2) = 2.75(2)$  Å), and the OH group is also involved in a hydrogen bond with the CO group of amide I of a neighboring dimer

Table IV. Comparison of Structural Features in Some Cofacial Porphyrin Dimers

compd	$d(\text{M}–\text{M}')$ (Å)	slippage <sup>a</sup> (Å)	slip angle <sup>b</sup> (deg)	interplanar distance (Å)	ref
$\text{Co}_2(\text{FTF4})$	3.417 (4)	0.13	2.2	3.54	this work
$\text{Ni}_2(\text{DPA})$	4.566	2.40	31.7	3.88	6
$\text{Cu}_2(\text{DPB})$	3.807	1.60	24.9	3.45	6
$\text{Cu}_2(\text{FTF6-3,2-}$ $\text{NH-diamide})$	6.332 (4)	4.95	51.4	3.87	c
$\text{Cu}_2(\text{DP7})^d$	5.22	3.80	46.4	3.52	e

<sup>a</sup> Most of the previous studies do not give a clear definition of the slippage. However, it is assumed to be similar to the one used in this study.<sup>11</sup> <sup>b</sup> Slip angle =  $\sin^{-1}(\text{slippage}/d(\text{M}–\text{M}'))$ . <sup>c</sup> Collman, J. P.; Chong, H. O.; Jameson, G. B.; Oakley, R. T.; Rose, E.; Schmittou, E. R.; Ibers, J. A. *J. Am. Chem. Soc.* **1981**, *103*, 516–533. <sup>d</sup> Diporphyrin with two seven-atom amide bridges. <sup>e</sup> Hatada, M. M.; Tulinsky, A.; Chang, C. K. *J. Am. Chem. Soc.* **1980**, *102*, 7115–7116.

molecule ( $\text{O}(\text{S}2)\cdots\text{O}(1) = 2.79(3)$  Å).

## Discussion

Table IV compares some structural features of the cofacial porphyrin dimers. They all show relatively short interplanar distances, presumably as a result of  $\pi$ – $\pi$  interactions between the porphyrin rings. However, the very slight slippage between the two metal centers of  $\text{Co}_2(\text{FTF4})$  makes this structure different, as in the other structures moderate to large slippage is found. In the present structure the two short rigid amide bridges at the transverse  $\beta$ -pyrrolic positions of the porphyrins apparently force the two rings to stack on top of each other.

In the FTF series, catalytic performance is very sensitive even to small changes in the amide bridges. For example, changing the number of atoms in the bridge by one (FTF5 and FTF3),<sup>2,3</sup> changing the position of the amide group in the bridge (FTF4\*),<sup>3</sup> or reduction of the amides to amines<sup>1b</sup> leads to significant loss of  $4e^-$  catalytic activity. Such changes in the bridges must induce changes in the metal–metal distance or in the relative orientation of the two rings or both. Thus the present  $\text{Co}_2(\text{FTF4})$  structure represents one possible “optimized” diporphyrin geometry for  $4e^-$  reduction of dioxygen. A crystallographic study<sup>6</sup> of  $\text{Ni}_2(\text{DPA})$  and  $\text{Cu}_2(\text{DPB})$  (which should have very similar structures to those of the catalytically effective bis-cobalt derivatives) showed the metal–metal separation in these two complexes to differ by 0.76 Å. It is therefore likely that  $\text{Co}_2(\text{DPA})$  and  $\text{Co}_2(\text{DPB})$  are  $4e^-$  catalysts by virtue of the flexibility<sup>18</sup> of their single link between the porphyrins, a conclusion shared by the authors.<sup>6</sup> Further structural work on the homologues of  $\text{Co}_2(\text{FTF4})$  is necessary to gain better understanding of the structure–function relationship and consequently of the mechanism of the catalytic  $4e^-$   $\text{O}_2$  reduction.

(18) The presumed flexibility of these singly bridged cofacial diporphyrins is supported by the synthesis of  $\text{M}_2(\text{DPB})$  ( $\text{M} = \text{Ru}$  or  $\text{Mo}$ ) in which there is an intramolecular metal–metal bond: Collman, J. P.; Kim, K.; Garner, J. M. *J. Chem. Soc., Chem. Commun.* **1987**, 1711–1713. To form such a bond requires considerable rearrangement of the conformation found in the solid-state structure of  $\text{Cu}_2(\text{DPB})$ .

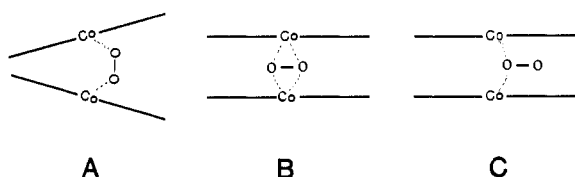


**Figure 7.** Three different modes of O<sub>2</sub> binding suggested for  $\mu$ -superoxo complex of four-atom-bridged cofacial dimer.

Another interesting property of the Co<sub>2</sub>(FTF4) system is the existence of a stable mixed-valence state, Co<sup>III</sup>Co<sup>II</sup>,<sup>19</sup> which now seems to be a consequence of the very short distance that promotes a strong interaction between the two nearly equivalent Co centers. The mixed-valence complex exhibits a very high O<sub>2</sub> affinity and forms a stable O<sub>2</sub><sup>-</sup> ( $\mu$ -superoxo) complex.<sup>20</sup> The role of this stable O<sub>2</sub><sup>-</sup> complex in the catalytic O<sub>2</sub> reduction is not fully understood, but its structure may further clarify the mechanism of this important process. Several years ago from the shape of the EPR spectrum of the  $\mu$ -superoxo complex, Chang and Wang proposed<sup>21</sup> that, in the four-atom-bridged dimer, dioxygen binds in a cis fashion (structure A in Figure 7). A theoretical study<sup>22</sup> suggests that such a cis structure may exist if steric constraints allow it. However, the present structure does not seem to support this hypothesis since enormous steric repulsion would result as the two

porphyrin rings approach one another on one side to accommodate a cis-bound O<sub>2</sub> complex. Instead, we suspect dioxygen may be bound between the Co centers parallel to the porphyrin rings either symmetrically (structure B) or asymmetrically (structure C in Figure 7). Although neither of these O<sub>2</sub> binding modes has been observed in transition-metal complexes,<sup>23</sup> structure B was once proposed in a theoretical study<sup>24</sup> for [(H<sub>3</sub>N)<sub>5</sub>Co]<sub>2</sub>O<sub>2</sub><sup>5+</sup>. Structure C is attractive since it makes the coordinated O<sub>2</sub> molecule more susceptible to protonation. Recently we isolated<sup>5</sup> the O<sub>2</sub> complexes of Co<sub>2</sub>(FTF4) and Co<sub>2</sub>(DPB), but thus far we have not been able to grow single crystals suitable for X-ray diffraction study. Therefore, the nature of O<sub>2</sub> bonding in these complexes remains unresolved at this time.

**Acknowledgment.** We thank Dr. M. G. Finn and Professor Brian M. Hoffman for helpful discussions. This work was kindly supported by the National Institutes of Health (HL-13157, JAI; 5R01-NIHGM17880-15,16, JPC) and by the National Science Foundation (NSF CHE83-18512, JPC).

**Registry No.** Co<sub>2</sub>(FTF4)·CH<sub>3</sub>OH·1.6CH<sub>2</sub>Cl<sub>2</sub>, 114221-01-1.

**Supplementary Material Available:** Positional and equivalent isotropic thermal parameters for non-hydrogen atoms (Table SI), anisotropic thermal parameters (Table SII), hydrogen-atom parameters (Table SIV), and least-squares planes and dihedral angles between the least-squares planes (Table SV) (4 pages); listing of observed and calculated structure amplitudes (Table SIII) (13 pages). Ordering information is given on any current masthead page.

(19) Le Mest, Y.; L'Her, M.; Courtot-Coupez, J.; Collman, J. P.; Evitt, E. R.; Bencosme, C. S. *J. Electroanal. Chem.* **1985**, *184*, 331-346.

(20) (a) Le Mest, Y.; L'Her, M.; Courtot-Coupez, J.; Collman, J. P.; Evitt, E. R.; Bencosme, C. S. *J. Chem. Soc., Chem. Commun.* **1983**, 1286-1287. (b) Le Mest, Y.; L'Her, M.; Collman, J. P.; Hendricks, N. H.; McElwee-White, L. *J. Am. Chem. Soc.* **1986**, *108*, 533-535.

(21) Change, C. K.; Wang, C.-B. In *Electron Transport and Oxygen Utilization*; Ho, C., Ed.; Elsevier: Amsterdam, 1982; pp 237-243.

(22) Tatsumi, K.; Hoffmann, R. *J. Am. Chem. Soc.* **1981**, *103*, 3328-3341.

(23) The symmetrically bridging side-on coordination geometry of dioxygen (Structure B) has been observed in a uranium complex. Boeyens, J. C. A.; Haeghele, R. *J. Chem. Soc., Dalton Trans.* **1977**, 648-650.

(24) Vlček, A. A. *Trans. Faraday Soc.* **1960**, *56*, 1137-1143.

## Synthesis of an ( $\eta^3$ -Allyl)(hydrido)iridium Complex and Its Reactions with Arenes and Alkanes. Sequential Intermolecular C-H Oxidative Addition and Hydride-to-Alkene Migratory Insertion Reactions

William D. McGhee and Robert G. Bergman\*

*Contribution from the Materials and Chemical Sciences Division, Lawrence Berkeley Laboratory, and the Department of Chemistry, University of California, Berkeley, California 94720.*

*Received November 2, 1987*

**Abstract:** The iridium allyl hydride complex ( $\eta^5$ -C<sub>5</sub>Me<sub>5</sub>)( $\eta^3$ -C<sub>3</sub>H<sub>5</sub>)(H)Ir (**2**) has been prepared from [( $\eta^5$ -C<sub>5</sub>Me<sub>5</sub>)IrCl<sub>2</sub>]<sub>2</sub>, and its reaction with arenes and alkanes has been investigated. The hydride reacts with C-H bonds in benzene and cyclopropane in the presence of phosphines L, leading to the phenyl and cyclopropyl complexes ( $\eta^5$ -C<sub>5</sub>Me<sub>5</sub>)(L)Ir(*n*-propyl)(R) (**3**, **4**, and **5**). Irradiation of **2** in the presence of PMe<sub>3</sub> takes a different course, giving the previously uncharacterized ( $\eta^5$ -C<sub>5</sub>Me<sub>5</sub>)Ir(PMe<sub>3</sub>)<sub>2</sub> (**6**). Thermal reaction of **2** in alkane solvents such as *n*-butane and isobutane, which are capable of  $\beta$ -elimination, leads to products **8a**, **8b**, and **9** formed by replacement of the allyl group in **2** by a substituted allyl ligand formed by overall dehydrogenation of the alkane. Thermolysis of **2** in the presence of arenes such as *n*-propylbenzene and cumene leads to more complicated products resulting from intermolecular C-H activation followed by cyclometalation (e.g., **13**, **15**) and/or dimerization (**20**). The structure of cyclometalated dimer **20** has been determined by X-ray diffraction. Mechanistic studies, including kinetics, isotope tracer experiments, and intra- versus intermolecular isotope effect determinations, implicate the coordinatively unsaturated species ( $\eta^5$ -C<sub>5</sub>Me<sub>5</sub>)( $\eta^2$ -propene)Ir (complex A in Scheme XX) as the initially formed intermediate in the thermal reactions of **1** with alkanes and arenes. Significant differences exist between the behavior of this intermediate (cf. Schemes XIX and XXIII) and that of the closely related phosphine-substituted complex ( $\eta^5$ -C<sub>5</sub>Me<sub>5</sub>)(PMe<sub>3</sub>)Ir studied earlier; possible reasons for these differences are discussed.

Many examples are now known of C-H activation by soluble transition-metal complexes.<sup>1</sup> In only a few systems, however,

has the product of C-H insertion been converted, either stoichiometrically or catalytically, into functionalized organic prod-